New transiting hot Jupiters discovered by WASP-South, Euler/CORALIE, and TRAPPIST-South

Coel Hellier,[1]★ D. R. Anderson [●],[1] F. Bouchy,[2] A. Burdanov,[3] A. Collier Cameron [●],[4]
L. Delrez,[3,5] M. Gillon,[3] E. Jehin,[3] M. Lendl [●],[6] L. D. Nielsen,[2] P. F. L. Maxted,[1]
F. Pepe,[2] D. Pollacco,[7] D. Queloz,[5] D. Ségransan,[2] B. Smalley [●],[1] A. H. M. J. Triaud,[8]
S. Udry[2] and R. G. West [●][7]

[1]*Astrophysics Group, Keele University, Staffordshire, ST5 5BG, UK*
[2]*Observatoire astronomique de l'Université de Genève 51 ch. des Maillettes, 1290 Sauverny, Switzerland*
[3]*Space sciences, Technologies and Astrophysics Research (STAR) Institute, Université de Liège, Allée du 6 Août, 17, Bat. B5C, 4000 Liège, Belgium*
[4]*SUPA, School of Physics and Astronomy, University of St. Andrews, North Haugh, Fife, KY16 9SS, UK*
[5]*Cavendish Laboratory, J J Thomson Avenue, Cambridge, CB3 0HE, UK*
[6]*Space Research Institute, Austrian Academy of Sciences, Schmiedlstr. 6, 8042, Graz, Austria*
[7]*Department of Physics, University of Warwick, Gibbet Hill Road, Coventry CV4 7AL, UK*
[8]*School of Physics & Astronomy, University of Birmingham, Edgbaston, Birmingham, B15 2TT, UK*

ABSTRACT

We report the discovery of eight hot-Jupiter exoplanets from the WASP-South transit survey. WASP-144b has a mass of 0.44 $M_{\rm Jup}$, a radius of 0.85 $R_{\rm Jup}$, and is in a 2.27-d orbit around a $V = 12.9$, K2 star which shows a 21-d rotational modulation. WASP-145Ab is a 0.89 $M_{\rm Jup}$ planet in a 1.77-d orbit with a grazing transit. The host is a $V = 11.5$, K2 star with a companion 5 arcsec away and 1.4 mag fainter. WASP-158b is a relatively massive planet at 2.8 $M_{\rm Jup}$ with a radius of 1.1 $R_{\rm Jup}$ and a 3.66-d orbit. It transits a $V = 12.1$, F6 star. WASP-159b is a bloated hot Jupiter (1.4 $R_{\rm Jup}$ and 0.55 $M_{\rm Jup}$) in a 3.8-d orbit around a $V = 12.9$, F9 star. WASP-162b is a massive planet in a relatively long and highly eccentric orbit (5.2 $M_{\rm Jup}$, $P = 9.6$ d, $e = 0.43$). It transits a $V = 12.2$, K0 star. WASP-168b is a bloated hot Jupiter (0.42 $M_{\rm Jup}$; 1.5 $R_{\rm Jup}$) in a 4.15-d orbit with a grazing transit. The host is a $V = 12.1$, F9 star. WASP-172b is a bloated hot Jupiter (0.5 $M_{\rm Jup}$; 1.6 $R_{\rm Jup}$) in a 5.48-d orbit around a $V = 11.0$, F1 star. WASP-173Ab is a massive planet (3.7 $M_{\rm Jup}$) with a 1.2 $R_{\rm Jup}$ radius in a circular orbit with a period of 1.39 d. The host is a $V = 11.3$, G3 star, being the brighter component of the double-star system WDS23366 − 3437, with a companion 6 arcsec away and 0.8 mag fainter. One of the two stars shows a rotational modulation of 7.9 d.

Key words: stars: individual (WASP-144, WASP-145A, WASP-158, WASP-159, WASP-162, WASP-168, WASP-172, WASP-173A) – planetary systems.

1 INTRODUCTION

Hot-Jupiter exoplanets are relatively rare, being found in only ∼1 per cent of Solar-like stars. However, since they are the easiest planets to detect they are by far the commonest type of planets found by ground-based transit surveys such as WASP (Pollacco et al. 2006). Such planets produce relatively deep transits (∼1 per cent) that recur often owing to short orbital periods (1–10 d). A massive planet in a close-in orbit will also produce a radial-velocity signal

large enough for verification with relatively small telescopes such as the Swiss Euler 1.2-m and its CORALIE spectrograph. The ease of studying hot Jupiters also makes them important targets for characterization. As an example, the community *Early Release Science* program for transiting exoplanets with the *James Webb Space Telescope* (Bean et al. 2018) has chosen WASP-18b, WASP-43b, and WASP-79b as the prime targets.

The imminent *TESS* satellite (Ricker et al. 2016) will perform an all-sky transit survey that is expected to find any hot Jupiters transiting bright stars that the ground-based surveys have missed. In the meantime, several ground-based surveys are making ongoing discoveries including HAT-South (e.g. Henning et al. 2018), KELT

★ E-mail: c.hellier@keele.ac.uk

(e.g. Johnson et al. 2018), MASCARA (e.g. Talens et al. 2017), and NGTS (e.g. Bayliss et al. 2017). Here, we report the latest hot-Jupiter discoveries from the WASP-South transit survey, verified with the Euler/CORALIE spectrograph (e.g. Triaud et al. 2013) and with follow-up photometry from EulerCAM (e.g. Lendl et al. 2012) and from the robotic TRAPPIST-South photometer (e.g. Gillon et al. 2013).

2 OBSERVATIONS

WASP-South is an array of eight cameras that, for the observations reported here, each consisted of a 200-mm, f/1.8 Canon lenses with a 2k × 2k CCD, giving a 7.8° × 7.8° field. The cameras are all on the same mount, which rasters a set of fields with a typical 10-min cadence, recording stars in the range $V = 9$–13. Processed photometry is accumulated in a central archive where the multiyear dataset on each star is searched for transits (see Collier Cameron et al. 2007b). After vetting of all candidates by eye, the best ones are sent for follow-up observations with TRAPPIST-South and Euler/CORALIE. The observations for each star are listed in Table 1. All of our methods are similar to those for previous WASP-South discovery papers (e.g. Hellier et al. 2014; Maxted et al. 2016; Hellier et al. 2017), and for this reason the presentation here is relatively concise.

3 SPECTRAL ANALYSIS

We report spectral analyses of the host stars made using the CORALIE spectra. Adopting methods as described by Doyle et al. (2013), we estimated the effective temperature, T_{eff}, from the H α line, and the surface gravity, log g, from Na I D and Mg I b lines. We also report an indicative spectral type deduced from the T_{eff} estimates. We report [Fe/H] values determined from equivalent-width measurements of unblended Fe I lines. The errors that we quote for the abundances take into account the uncertainties in T_{eff} and log g. The Fe I lines were also used to estimate the rotation speed, $v\sin i$, after convolving with the CORALIE instrumental resolution ($R = 55\,000$), and also combining with an estimate of the macroturbulence take from Doyle et al. (2014). Lastly, we report lithium abundance values and corresponding age estimates using Sestito & Randich (2005), though such estimates are unreliable. The parameters obtained from the analysis are given in the tables for each system. Where available, we also list parallax values from the GAIA DR1 (Gaia Collaboration et al. 2016) and proper motions from the UCAC5 catalogue (Zacharias, Finch & Frouard 2017).

4 STELLAR ROTATIONAL MODULATIONS

The WASP photometry can span months of a year with observations on each clear night, and so is sensitive to rotational modulations down to the millimag level. We thus routinely search the photometry of planet hosts using a sine-wave fitting algorithm. We also compute a false alarm probability by repeatedly shuffling the nightly datasets (see Maxted et al. 2011). For most of the planet hosts in this paper we find only upper limits, but for WASP-144 and WASP-173 we found significant modulations.

5 SYSTEM PARAMETERS

As we have routinely done for previous planet-discovery papers, we combine the photometric and radial-velocity data sets for

Table 1. Observations.

Facility	Date	Notes
WASP-144:		
WASP-South	2006 May–2012 Jun	29 500 points
CORALIE	2014 Jun–2016 Oct	16 RVs
TRAPPIST	2014 Aug 13	Blue-block
TRAPPIST	2014 Nov 17	Blue-block
TRAPPIST	2015 May 18	Blue-block
TRAPPIST	2014 Jun 12	Blue-block
EulerCAM	2015 Jun 28	*NGTS* filter
WASP-145:		
WASP-South	2008 Jun–2012 Jun	54 000 points
CORALIE	2014 Jun–2016 Aug	19 RVs
TRAPPIST	2014 Nov 09	*z* band
EulerCAM	2014 Nov 16	Gunn *z* filter
EulerCAM	2015 Jul 02	Gunn *z* filter
WASP-158:		
WASP-South	2008 Jun–2012 Nov	27 000 points
CORALIE	2014 Aug–2016 Oct	20 RVs
TRAPPIST	2016 Oct 12	*I* + *z* band
EulerCAM	2016 Nov 03	*NGTS* filter
WASP-159:		
WASP-South	2006 Sep–2012 Feb	43 800 points
CORALIE	2014 Nov–2017 Mar	29 RVs
EulerCAM	2016 Dec 02	*NGTS* filter
WASP-162:		
WASP-South	2006 May–2012 Jun	37 400 points
CORALIE	2014 Apr–2017 May	18 RVs
TRAPPIST	2015 Jun 07	*I* + *z* band
EulerCAM	2017 Jan 14	I_c filter
WASP-168:		
WASP-South	2006 Oct–2012 Mar	31 000 points
CORALIE	2014 Dec–2017 Apr	31 RVs
TRAPPIST	2016 Feb 05	*I* + *z* band
TRAPPIST	2016 Sep 16	*V* band
EulerCAM	2016 Sep 16	I_c filter
WASP-172:		
WASP-South	2006 May–2012 Jun	35 000 points
CORALIE	2012 Apr–2017 Jun	38 RVs
TRAPPIST	2014 Feb 03	*I* + *z* band
TRAPPIST	2014 Jun 20	*I* + *z* band
EulerCAM	2015 Jul 03	Gunn *r* filter
TRAPPIST	2015 May 31	$z^{'}$ filter
WASP-173:		
WASP-South	2006 May–2011 Nov	19 000 points
CORALIE	2015 Sep–2016 Dec	18 RVs
EulerCAM	2016 Sep 21	Gunn *z* filter
TRAPPIST	2016 Oct 06	*V* filter
EulerCAM	2016 Oct 20	Gunn *z* filter

each system into one Markov-chain Monte Carlo (MCMC) analysis, using a code originally described by Collier Cameron et al. (2007a). Since the CORALIE spectrograph underwent an upgrade in 2014 November, we allow for a radial-velocity offset between the datasets before and after the upgrade (for future reference the RV values are listed in Table A1, where the time of upgrade is marked by a short line). The treatment of limb darkening is crucial to fitting transit photometry, and here we have used the four-parameter, non-linear law of Claret (2000), interpolating coefficients for the appropriate stellar temperature and metallicity of each star.

On early MCMC runs, we allowed the eccentricity to be a free parameter, and for one of our systems (WASP-162b) we found a highly significant eccentricity. Where, however, the outcome was

Table 2. Mass and age estimates for the host stars, derived from the BAGEMASS code with GARSTEC stellar models and assuming $\alpha_{MLT} = 1.78$. Columns 2–4 give the maximum-likelihood estimates of the age, mass, and initial metallicity, respectively. Column 5 is the chi-squared statistic of the fit for the parameter values in columns 2–4. Columns 6 and 7 give the mean and standard deviation of their posterior distributions. The systematic errors on the mass and age due to uncertainties in the mixing length and helium abundance are given in columns 8–11.

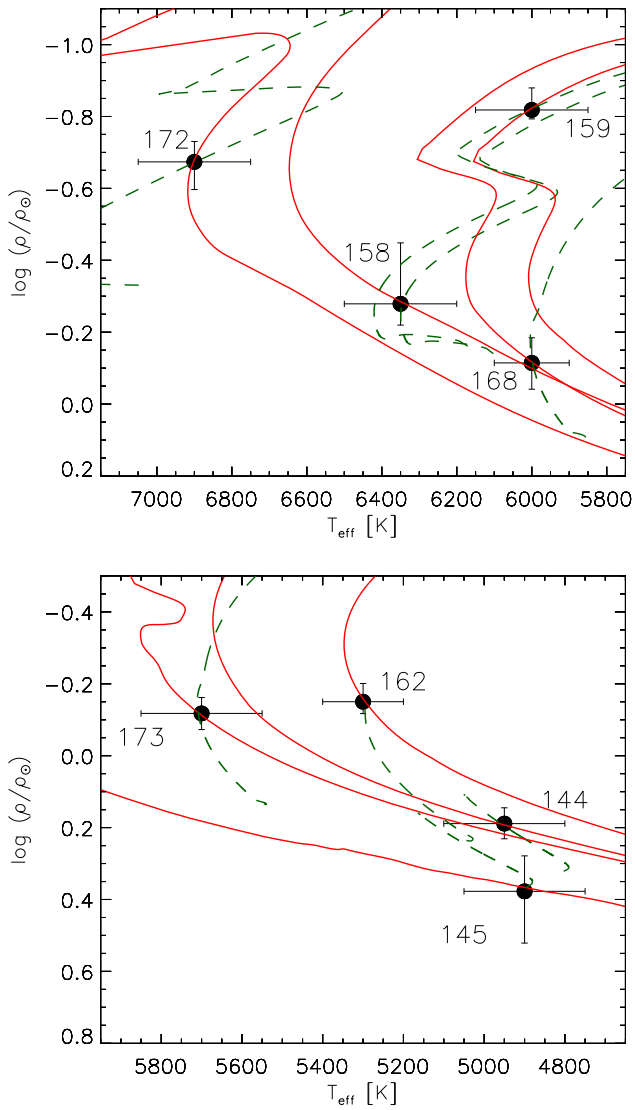| Star	$\tau_{iso,b}$ (Gyr)	M_b ($M_\odot$)	[Fe/H]$_{i,b}$	χ^2	$\langle\tau_{iso}\rangle$ (Gyr)	$\langle M_\star\rangle$ ($M_\odot$)	$\sigma_{\tau,Y}$	$\sigma_{\tau,\alpha}$	$\sigma_{M,Y}$	$\sigma_{M,\alpha}$
WASP-144	9.5	0.84	+0.238	0.01	8.71 ± 4.12	0.844 ± 0.046	1.96	3.96	−0.040	−0.026
WASP-145	0.0	0.79	− 0.048	0.07	6.99 ± 4.40	0.763 ± 0.040	0.12	0.02	−0.034	−0.006
WASP-158	1.5	1.32	+0.252	0.01	1.93 ± 0.93	1.339 ± 0.092	0.01	0.75	−0.035	−0.030
WASP-159	4.1	1.33	+0.227	0.03	3.40 ± 0.95	1.431 ± 0.118	− 0.08	1.04	−0.036	−0.103
WASP-162	13.7	0.94	+0.381	0.00	12.97 ± 2.35	0.953 ± 0.041	0.84	3.10	−0.044	−0.034
WASP-168	3.9	1.08	+0.046	0.01	3.96 ± 1.77	1.073 ± 0.053	0.35	1.65	−0.043	−0.034
WASP-172	1.7	1.48	− 0.102	0.04	1.79 ± 0.28	1.472 ± 0.067	0.00	0.03	−0.050	−0.006
WASP-173	6.6	1.03	+0.225	0.00	6.78 ± 2.93	1.035 ± 0.072	0.51	2.35	−0.044	−0.037

Figure 1. The host star's effective temperature (T_{eff}) versus density (each symbol being labelled by the WASP planet number). We show best-fitting evolution tracks (dashed lines) and isochrones (solid lines) for the masses, ages, and [Fe/H] values listed in Table 2.
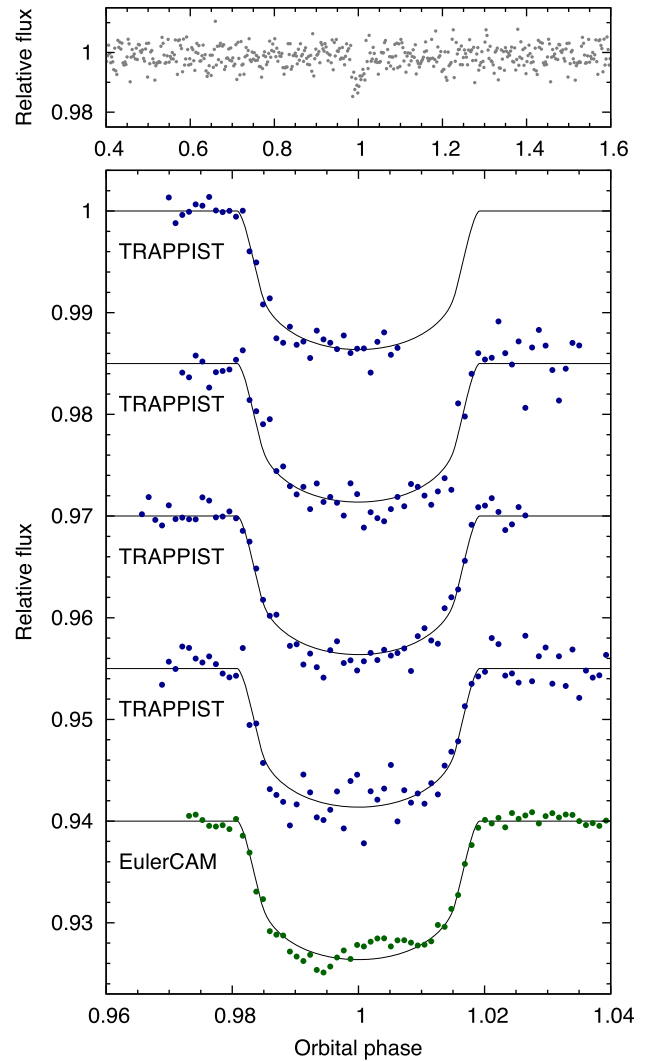

Figure 2. WASP-144b discovery photometry: (Top) The WASP data folded on the transit period. (Second panel) The binned WASP data with (offset) the follow-up transit light curves (ordered from the top as in Table 1) together with the fitted MCMC model.
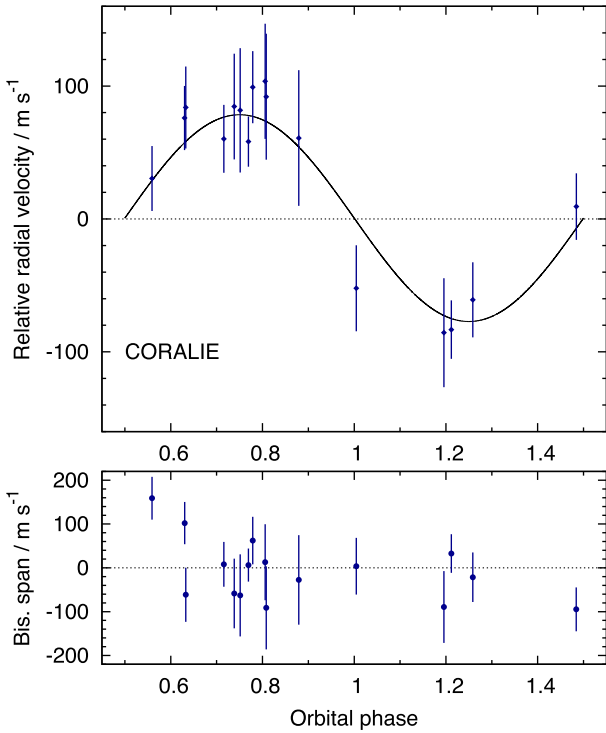
Figure 3. WASP-144b radial velocities and fitted model (top) along with (bottom) the bisector spans; the absence of any correlation with radial velocity is a check against transit mimics.

Table 3. System parameters for WASP-144.

1SWASP J212303.08–400253.6	
2MASS 21230309–4002537	
GAIA RA = $21^h23^m03.09^s$, Dec = $-40°02'54.4''$ (J2000)	
V mag = 12.9	
Rotational modulation: $P = 21 \pm 1$ d, 4–8 mmag	
UCAC5 pm (RA) -3.4 ± 1.0 (Dec) -41.7 ± 1.0 mas yr^{-1}	
Stellar parameters from spectroscopic analysis.	
Spectral type	K2V
T_{eff} (K)	$4\,950 \pm 150$
Log g	4.5 ± 0.2
$v \sin i$ (km s^{-1})	1.9 ± 1.2
[Fe/H]	$+0.18 \pm 0.14$
Log A(Li)	<0.6
Age (Lithium) (Gyr)	>0.5
Parameters from MCMC analysis.	
P (d)	$2.278\,315\,2 \pm 0.000\,001\,3$
T_c (HJD) (UTC)	$2\,45\,7\,157.274\,93 \pm 0.000\,15$
T_{14} (d)	$0.081\,4 \pm 0.000\,7$
$T_{12} = T_{34}$ (d)	$0.010\,4 \pm 0.000\,9$
$\Delta F = R_P^2/R_*^2$	$0.011\,65 \pm 0.000\,28$
b	0.45 ± 0.07
i (°)	86.9 ± 0.5
K_1 (km s^{-1})	0.078 ± 0.011
γ (km s^{-1})	16.105 ± 0.008
e	0 (adopted) (<0.30 at 2σ)
a/R_*	8.39 ± 0.23
M_* (M$_\odot$)	0.81 ± 0.04
R_* (R$_\odot$)	0.81 ± 0.04
Log g_* (cgs)	4.53 ± 0.03
ρ_* ($\rho_\odot$)	1.54 ± 0.16
T_{eff} (K)	$5\,200 \pm 140$
M_P (M$_{Jup}$)	0.44 ± 0.06
R_P (R$_{Jup}$)	0.85 ± 0.05
Log g_P (cgs)	3.15 ± 0.06
ρ_P (ρ_J)	0.72 ± 0.15
a (AU)	$0.031\,6 \pm 0.000\,5$
$T_{P,A=0}$ (K)	1260 ± 40

Note. Errors are 1σ; limb-darkening coefficients were:
r band: a1 = 0.734, a2 = -0.714, a3 = 1.399, a4 = -0.614.

compatible with a circular orbit, we then computed results with a circular orbit imposed (this gives the most likely set of parameters, as discussed by Anderson et al. (2012), essentially feeding in the prior expectation that most hot Jupiters have orbits that have been circularised by tidal forces).

The list of MCMC parameters for the circular-orbit case is T_c (the epoch of mid-transit), P (the orbital period), ΔF (the transit depth that would be observed in the absence of limb-darkening), T_{14} (duration from first to fourth contact), b (the impact parameter), and K_1 (the stellar reflex velocity). The fitted parameters and other values derived from them are listed in a table for each system, along with 1σ errors (though where no eccentricity is found we quote 2σ upper limits). Red noise in the photometry could mean that the uncertainties are larger than quoted. For an account of the effects of red noise in datasets similar to those reported here, see the analysis of multiple different transit light curves of WASP-36b by Smith et al. (2012).

An additional constraint on the fitting, continuing our practice from other recent discovery papers, comes from stellar models. We first run an MCMC analysis to estimate the stellar density (which can be derived from the transit light curve independently of a stellar model). We then use the stellar density and the spectroscopic effective temperature and metallicity to estimate the most likely stellar mass using the BAGEMASS code described in Maxted, Serenelli & Southworth (2015), which is based on the GARSTEC stellar evolution code (Weiss & Schlattl 2008). We then use a resulting stellar-mass estimate and its error as a Gaussian-prior input to the final MCMC analysis.

The masses and ages of the stars derived from BAGEMASS are given in Table 2. The best-fitting stellar evolution tracks and isochrones are shown in Fig. 1.

6 WASP-144

The discovery photometry and radial-velocity data for WASP-144 are shown in Figs 2 and 3. We also show the bisector spans, which are a check for transit mimics. The system parameters are listed in Table 3. WASP-144 is a relatively faint, $V = 12.9$, K2 star with a metallicity of [Fe/H] = $+0.18 \pm 0.14$. Evolutionary tracks suggest that it could be 8 ± 4 Gyr old (Table 2).

The WASP data show a possible rotational modulation at a period of 21 ± 1 d with an amplitude of 4–8 mmag (see Fig. 4). This is seen independently in data from the seasons 2006 (7 mmag amplitude; false-alarm probability <0.1 per cent), 2011 (4-mmag amplitude; FAP 6 per cent) and 2012 (8-mmag amplitude, FAP <0.1 per cent). The rotational period and fitted radius (0.81 ± 0.04 R$_\odot$) imply a surface rotational velocity of 1.96 ± 0.13 km s^{-1}, which compares with an observed $v\sin i$ of 1.9 ± 1.2 km s^{-1}. Thus, this is likely to be an aligned system (with the stellar spin axis perpendicular to us).

The follow-up photometry consists of four TRAPPIST-South transits and one from EulerCAM. The latter was observed in poor conditions with variable seeing, leading to systematic features in the light curve that we do not think are astrophysically real. The MCMC process down-weighted this light curve in the fitting.
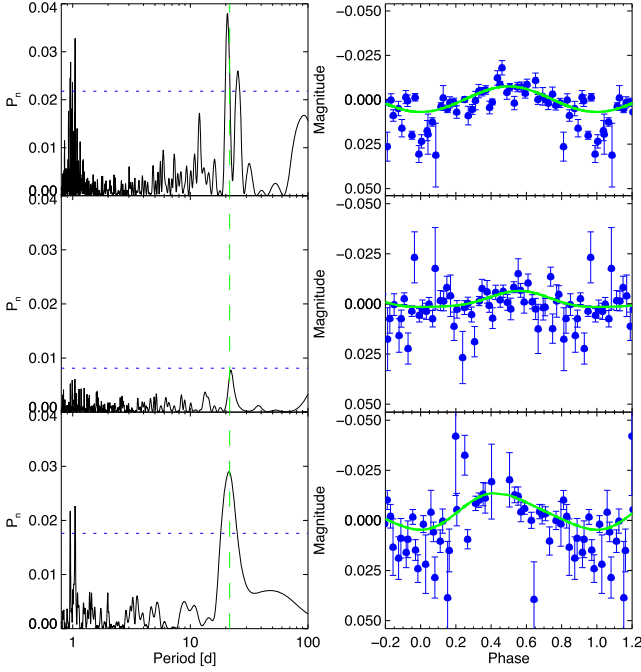
Figure 4. WASP-144 rotational modulation. The left-hand panels show periodograms for independent WASP-South data sets from 2006, 2011, and 2012. The blue dotted line is a false-alarm probability of 0.001. The right-hand panels show the data for each season folded on the 21-d period; the green line is a harmonic-series fit.
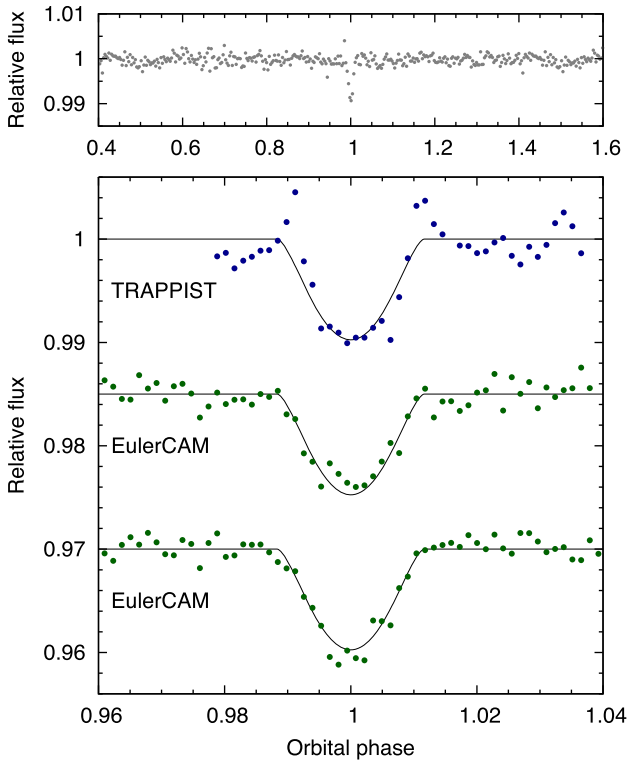

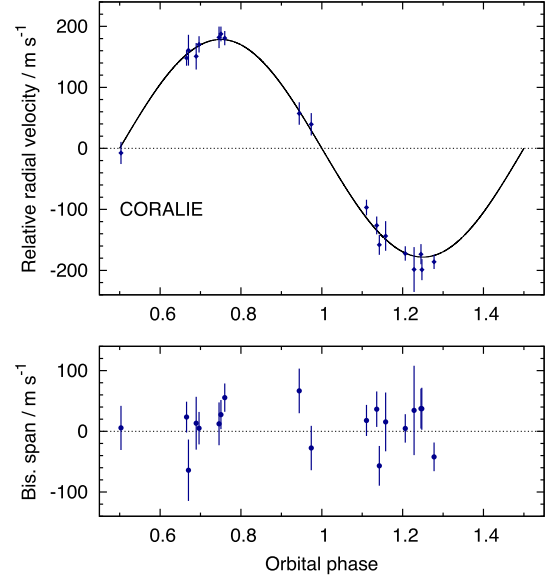**Figure 5.** WASP-145b discovery photometry, as for Fig. 2.

Figure 6. WASP-145b radial velocities and bisector spans, as for Fig. 3.

Table 4. System parameters for WASP-145.

1SWASP J212900.65–585008.4	
2MASS 212900.65–585008.4	
GAIA RA $= 21^h29^m00.90^s$, Dec $= -58°50'10.1''$ (J2000)	
V mag $= 11.5$	
Rotational modulation <2 mmag (95%)	
UCAC4 pm (RA) 102.6 ± 1.2 (Dec) 4.9 ± 3.4 mas yr^{-1}	

Stellar parameters from spectroscopic analysis.	
Spectral type	K2V
$T_{\rm eff}$ (K)	$4\,900 \pm 150$
Log g	4.6 ± 0.2
$v \sin i$ (km s^{-1})	2.1 ± 1.1
[Fe/H]	-0.04 ± 0.10
Log A(Li)	<0.5
Age (Lithium) (Gyr)	>0.5

Parameters from MCMC analysis.	
P (d)	$1.769\,038\,1 \pm 0.000\,000\,8$
$T_{\rm c}$ (HJD) (UTC)	$2\,45\,6\,844.165\,26 \pm 0.000\,26$
T_{14} (d)	0.0407 ± 0.0016
$T_{12} = T_{34}$ (d)	Undefined
$\Delta F = R_{\rm P}^2/R_*^2$	$0.011\,6 \pm 0.002\,6$
b	0.97 ± 0.09
i (°)	83.3 ± 1.3
K_1 (km s^{-1})	0.178 ± 0.006
γ (km s^{-1})	3.345 ± 0.005
e	0 (adopted) (<0.06 at 2σ)
a/R_*	8.74 ± 0.52
M_* (M$_\odot$)	0.76 ± 0.04
R_* (R$_\odot$)	0.68 ± 0.07
Log g_* (cgs)	4.65 ± 0.10
ρ_* ($\rho_\odot$)	2.38 ± 0.93
$T_{\rm eff}$ (K)	$4\,900 \pm 150$
$M_{\rm P}$ ($M_{\rm Jup}$)	0.89 ± 0.04
$R_{\rm P}$ ($R_{\rm Jup}$)	0.9 ± 0.4
Log $g_{\rm P}$ (cgs)	3.4 ± 0.4
$\rho_{\rm P}$ ($\rho_{\rm J}$)	1.2 ± 1.0
a (AU)	$0.026\,1 \pm 0.000\,5$
$T_{\rm P,A\,=\,0}$ (K)	$1\,200 \pm 60$

Note. Errors are 1σ; limb-darkening coefficients were:
r band: a1 $= 0.703$, a2 $= -0.734$, a3 $= 1.472$, a4 $= -0.630$.
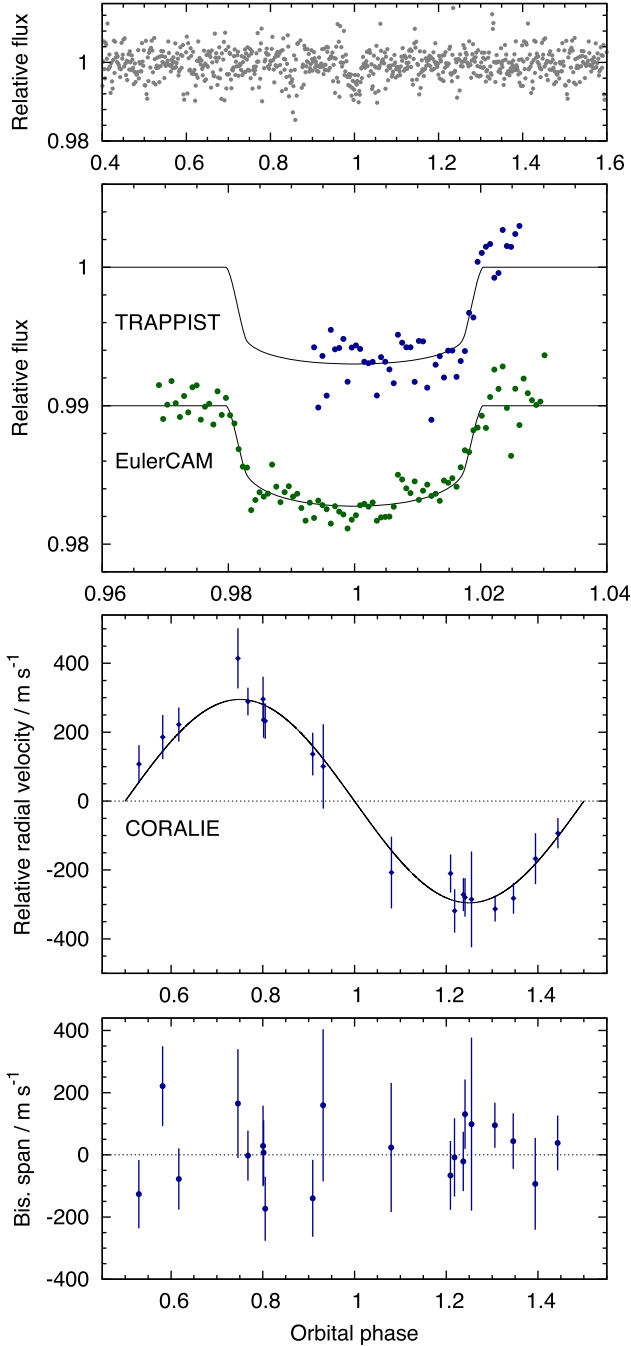z band: a1 $= 0.765$, a2 $= -0.800$, a3 $= 1.258$, a4 $= -0.530$.

Figure 7. WASP-158b discovery data, as for Figs 2 and 3.

Table 5. System parameters for WASP-158.

1SWASP J001635.09–105834.9	
2MASS 001635.09–105834.9	
GAIA RA = $00^h16^m35.12^s$, Dec = $-10°58'35.1''$ (J2000)	
V mag = 12.1	
Rotational modulation <1.5 mmag (95%)	
UCAC5 pm (RA) 2.4 ± 1.2 (Dec) 0.4 ± 1.2 mas yr^{-1}	
GAIA DR1 parallax: 0.88 ± 0.57 mas	
Stellar parameters from spectroscopic analysis.	
Spectral type	F6V
$T_{\rm eff}$ (K)	$6\,350 \pm 150$
Log g	4.5 ± 0.2
$v \sin i$ (km s^{-1})	9.3 ± 1.3
[Fe/H]	$+0.24 \pm 0.10$
Log A(Li)	<1.7
Age (Lithium) (Gyr)	(Close to Lithium gap)
Parameters from MCMC analysis.	
P (d)	$3.656\,333 \pm 0.000\,004$
$T_{\rm c}$ (HJD) (UTC)	$2\,45\,7\,619.9195 \pm 0.001\,0$
T_{14} (d)	$0.149\,0 \pm 0.003\,7$
$T_{12} = T_{34}$ (d)	0.014 ± 0.002
$\Delta F = R_{\rm P}^2/R_*^2$	$0.006\,3 \pm 0.000\,5$
b	0.32 ± 0.23
i (°)	87.7 ± 1.5
K_1 (km s^{-1})	0.295 ± 0.015
γ (km s^{-1})	24.197 ± 0.012
e	0 (adopted) (<0.16 at 2σ)
a/R_*	$8.0^{+0.4}_{-1.0}$
M_* (M$_\odot$)	1.38 ± 0.14
R_* (R$_\odot$)	1.39 ± 0.18
Log g_* (cgs)	$4.30^{+0.05}_{-0.11}$
ρ_* ($\rho_\odot$)	$0.53^{+0.08}_{-0.17}$
$T_{\rm eff}$ (K)	$6\,350 \pm 150$
$M_{\rm P}$ (M$_{\rm Jup}$)	2.79 ± 0.23
$R_{\rm P}$ (R$_{\rm Jup}$)	1.07 ± 0.15
Log $g_{\rm P}$ (cgs)	$3.75^{+0.06}_{-0.14}$
$\rho_{\rm P}$ ($\rho_{\rm J}$)	$2.3^{+0.5}_{-0.9}$
a (AU)	$0.051\,7 \pm 0.001\,8$
$T_{\rm P,A=0}$ (K)	$1\,590 \pm 80$

Note. Errors are 1σ; limb-darkening coefficients were:
r band: a1 = 0.568, a2 = 0.137, a3 = 0.145, a4 = −0.136.
z band: a1 = 0.658, a2 = −0.252, a3 = 0.422, a4 = −0.226.

WASP-144b has a mass of 0.44 $M_{\rm Jup}$ and a radius of 0.85 $R_{\rm Jup}$ and is in a 2.27-d orbit. The radius of 0.85 $R_{\rm Jup}$ is among the lowest found for hot-Jupiter planets. Comparable planets are WASP-60b (0.50 $M_{\rm Jup}$; 0.90 $R_{\rm Jup}$; Hébrard et al. 2013a) and Kepler-41b (0.55 $M_{\rm Jup}$; 0.89 $R_{\rm Jup}$; Santerne et al. 2011). Both of those have G-star hosts whereas WASP-144 is a K2 star.

7 WASP-145

WASP-145A is a $V = 11.5$, K2 star, with solar metallicity ([Fe/H] = +0.04 ± 0.10) and an estimated age of 7 ± 4 Gyr (Figs 5 and 6; Table 4).

WASP-145A has a companion star, WASP-145B, separated by 5.14 ± 0.01 arcsec with a position angle of −5.04 ± 0.13 degrees, and fainter by 1.407 ± 0.009 mag (as measured by focused EulerCAM images in a z'-band filter). It is likely that this star is physically associated with WASP-145A, but this is not certain. The later EulerCAM light curve (2015 July) was extracted using an aperture including both stars and this light curve was corrected for dilution in the analysis (the other follow-up light curves used a smaller aperture containing only the host star).

The planet WASP-145Ab has a 1.77-d orbit and a grazing transit ($b = 0.97 \pm 0.09$), which means that 2$^{\rm nd}$ and 3$^{\rm rd}$ contact are not discernable and thus that the planetary radius is not well constrained. We estimate the mass at 0.89 ± 0.04 $M_{\rm Jup}$ and the radius at 0.9 ± 0.4 $R_{\rm Jup}$. If the radius were at the lower end of that range it would be abnormally low for a hot Jupiter. The transit depth of 1.1 per cent is typical for a hot Jupiter owing to a relatively small stellar radius of 0.68 ± 0.07 R$_\odot$.
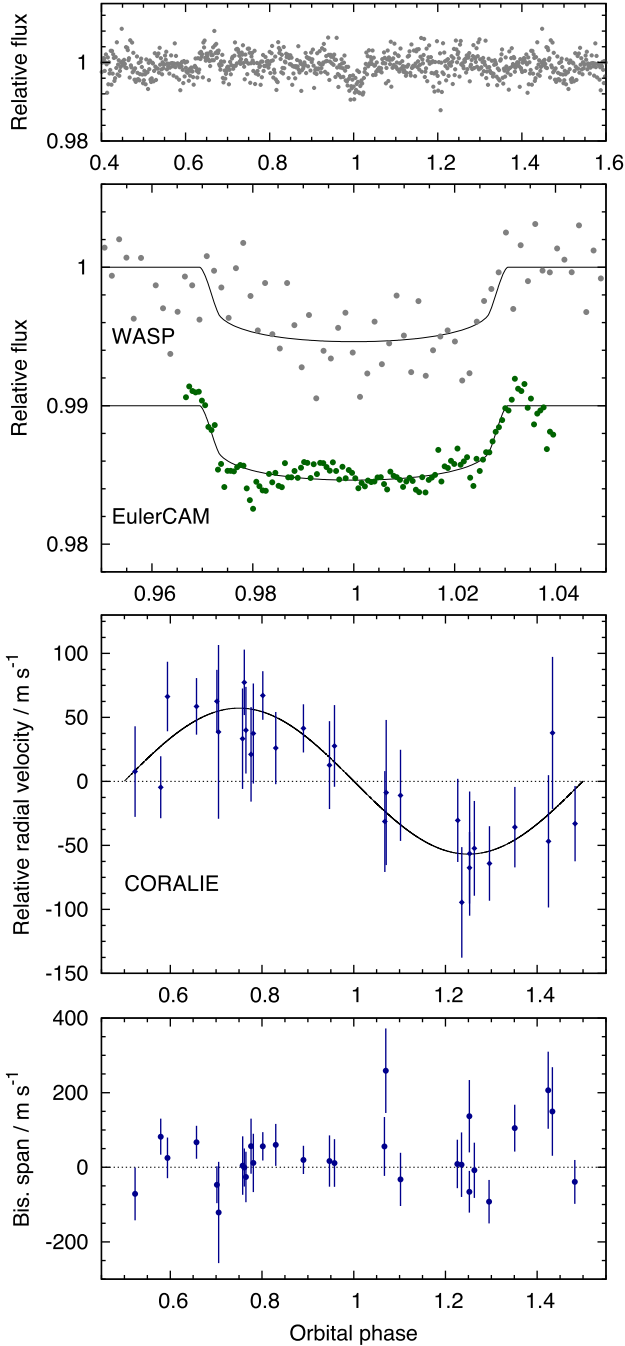
Figure 8. WASP-159b discovery data as for Figs 2 and 3.

Table 6. System parameters for WASP-159.

1SWASP J043232.73–385805.8	
2MASS 04323274–3858060	
GAIA RA = $04^h32^m32.76^s$, Dec = $-38°58'06.0''$ (J2000)	
V mag = 12.8	
Rotational modulation <1.5 mmag (95%)	
UCAC5 pm (RA) -0.9 ± 1.0 (Dec) 5.2 ± 1.0 mas yr^{-1}	
GAIA parallax: 1.08 ± 0.24 mas	
Stellar parameters from spectroscopic analysis.	
Spectral type	F9
T_{eff} (K)	6000 ± 150
Log g	4.0 ± 0.1
$v \sin i$ (km s^{-1})	5.7 ± 0.4
[Fe/H]	$+0.22 \pm 0.12$
Log A(Li)	2.15 ± 0.12
Age (Lithium) (Gyr)	2 to 8
Parameters from MCMC analysis.	
P (d)	$3.840\,401 \pm 0.000\,007$
T_c (HJD) (UTC)	$2\,45\,7\,668.084\,9 \pm 0.000\,9$
T_{14} (d)	$0.232\,8 \pm 0.002\,1$
$T_{12} = T_{34}$ (d)	$0.015\,2 \pm 0.001\,6$
$\Delta F = R_P^2/R_*^2$	$0.004\,53 \pm 0.000\,18$
b	0.18 ± 0.15
i (°)	88.1 ± 1.4
K_1 (km s^{-1})	0.057 ± 0.008
γ (km s^{-1})	35.160 ± 0.006
e	0 (adopted) (<0.18 at 2σ)
a/R_*	$5.44^{+0.15}_{-0.29}$
M_* (M$_\odot$)	1.41 ± 0.12
R_* (R$_\odot$)	2.11 ± 0.10
Log g_* (cgs)	3.94 ± 0.04
ρ_* ($\rho_\odot$)	0.15 ± 0.02
T_{eff} (K)	6120 ± 140
M_P (M_{Jup})	0.55 ± 0.08
R_P (R_{Jup})	1.38 ± 0.09
Log g_P (cgs)	2.82 ± 0.07
ρ_P (ρ_J)	0.21 ± 0.04
a (AU)	$0.053\,8 \pm 0.001\,5$
$T_{P, A=0}$ (K)	$1\,850 \pm 50$

Note. Errors are 1σ; limb-darkening coefficients were:
r band: a1 = 0.595, a2 = 0.011, a3 = 0.345, a4 = −0.220.

9 WASP-159

WASP-159 (Fig. 8; Table 6) is a fainter, $V = 12.9$, F9 star with a metallicity of [Fe/H] = $+0.22 \pm 0.12$. It appears to be evolving off the main sequence with a radius of 2.1 ± 0.1 R$_\odot$ and an age estimate of 3.4 ± 1.0 Gyr (Fig. 1; Table 2).

The fact that the stellar radius is expanded means that the transit depth is relatively small for a transiting hot Jupiter at 0.45 per cent. This depth still equates to a fairly bloated planet (1.4 R_{Jup} and 0.55 M_{Jup}). This is a well-populated region of a hot-Jupiter mass–radius plot, no doubt in part because bloated planets are easiest to find in ground-based transit surveys.

10 WASP-162

WASP-162 is a $V = 12.2$, K0 star with a metallicity of [Fe/H] = $+0.28 \pm 0.13$. It appears to be old, with an expanded radius for a low-mass star ($R = 1.11 \pm 0.05$ R$_\odot$; $M = 0.95 \pm 0.05$ M$_\odot$) leading to an age estimate of 13 ± 2 Gyr. This star may have an inflated radius owing to magnetic activity. This phenomenon can be
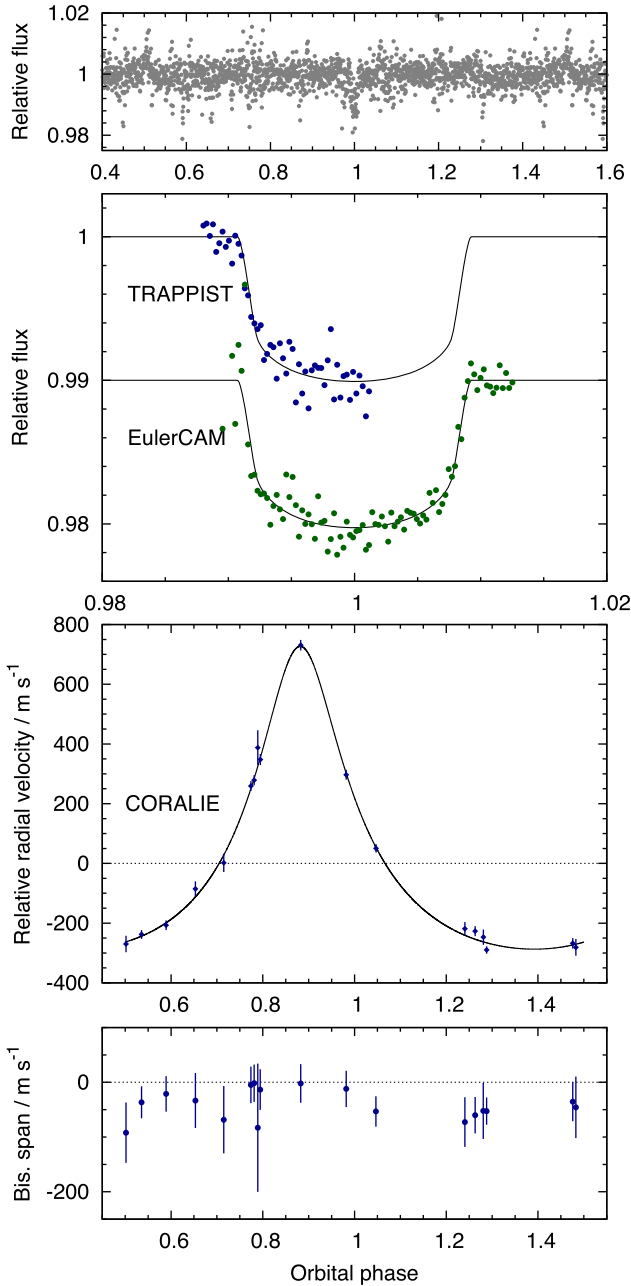
8 WASP-158

WASP-158 is a $V = 12.1$, F6 star with a metallicity of [Fe/H] = $+0.24 \pm 0.15$. It is compatible with being an unevolved main-sequence star with an age estimate of 1.9 ± 0.9 Gyr.

The planet, WASP-158b, is relatively massive at 2.8 M_{Jup} with a radius of 1.1 R_{Jup}, and has a 3.66-d orbit (Fig. 7; Table 5). WASP-158b is thus very similar to WASP-38b (2.7 M_{Jup}; 1.1 R_{Jup}, in a 6.9-d orbit around an F8 star; Barros et al. 2011) and WASP-99b (2.8 M_{Jup}; 1.1 R_{Jup}, in a 5.8-d orbit around an F8 star; Hellier et al. 2014).

Figure 9. WASP-162b discovery data, as for Figs 2 and 3.

Table 7. System parameters for WASP-162.

1SWASP J111310.29–173928.1	
2MASS 11131028–1739280	
GAIA RA = $11^h13^m10.30^s$, Dec = $-17°39'28.0''$ (J2000)	
V mag = 12.2	
Rotational modulation <1 mmag (95%)	
UCAC5 pm (RA) 6.2 ± 1.2 (Dec) -8.1 ± 1.2 mas yr^{-1}	

Stellar parameters from spectroscopic analysis.	
Spectral type	K0
$T_{\rm eff}$ (K)	$5\,300 \pm 100$
Log g	4.5 ± 0.1
$v \sin i$ (km s^{-1})	1.0 ± 0.8
[Fe/H]	$+0.28 \pm 0.13$
Log A(Li)	<0.7
Age (Lithium) (Gyr)	>1

Parameters from MCMC analysis.	
P (d)	$9.624\,68 \pm 0.000\,01$
T_c (HJD) (UTC)	$2\,45\,7\,701.3816 \pm 0.000\,6$
T_{14} (d)	$0.177\,4 \pm 0.001\,5$
$T_{12} = T_{34}$ (d)	0.016 ± 0.001
$\Delta F = R_p^2/R_*^2$	$0.008\,7 \pm 0.000\,3$
b	0.18 ± 0.14
i (°)	89.3 ± 0.5
K_1 (km s^{-1})	0.507 ± 0.008
γ (km s^{-1})	16.824 ± 0.004
e	0.434 ± 0.005
ω (deg)	-1.9 ± 2.2
a/R_*	$17.0^{+0.4}_{-0.6}$
M_* (M$_\odot$)	0.95 ± 0.04
R_* (R$_\odot$)	1.11 ± 0.05
log g_* (cgs)	4.33 ± 0.03
ρ_* ($\rho_\odot$)	0.71 ± 0.07
$T_{\rm eff}$ (K)	$5\,300 \pm 100$
M_P (M$_{\rm Jup}$)	5.2 ± 0.2
R_P (R$_{\rm Jup}$)	1.00 ± 0.05
Log g_P (cgs)	4.33 ± 0.03
ρ_P (ρ_J)	5.2 ± 0.6
a (AU)	$0.087\,1 \pm 0.001\,3$
$T_{P, A = 0}$ (K)	910 ± 20

Note. Errors are 1σ; limb-darkening coefficients were:
r band: a1 = 0.750, a2 = −0.724, a3 = 1.393, a4 = −0.614.
z band: a1 = 0.826, a2 = −0.863, a3 = 1.266, a4 = −0.540.
I band: a1 = 0.827, a2 = −0.881, a3 = 1.376, a4 = −0.598.

Comparable high-mass, long-period hot Jupiters in eccentric orbits include WASP-8b (2.2 $M_{\rm Jup}$, 8.2 d, $e = 0.31$; Queloz et al. 2010) and Kepler-75 (9.9 $M_{\rm Jup}$, 8.9 d, $e = 0.57$; Hébrard et al. 2013b).

11 WASP-168

WASP-168 (Figs 10 and 11; Table 8) is a $V = 12.1$, F9 star with a metallicity of [Fe/H] $= -0.01 \pm 0.09$. The evolutionary tracks indicate an age of 4 ± 2 Gyr. The lithium abundance of log A(Li) 2.93 ± 0.12 indicates an age of <1 Gyr, though we consider this less reliable.

The planet has a 4.15-d orbit. Of the three follow-up transit light curves, note that the EulerCAM transit was observed simultaneously by TRAPPIST-South. These all show a grazing transit with a high impact factor ($b = 0.97 \pm 0.05$). As with WASP-145Ab, this means that the 2nd and 3rd contact are not discernable and thus that the
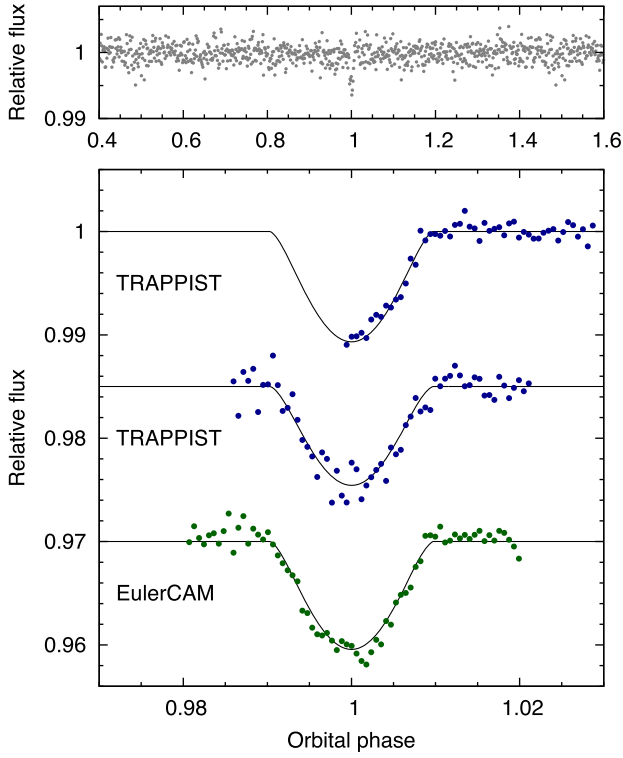
accounted for to some extent by using models with a lower mixing-length parameter ($\alpha_{\rm MLT}$). If we assume $\alpha_{\rm MLT} = 1.50$ for this star instead of standard value of $\alpha_{\rm MLT} = 1.78$ from a solar calibration, we obtain a best-fitting age of 9.2 Gyr.

The planet is massive, at 5.2 ± 0.2 $M_{\rm Jup}$, and is in a relatively long and eccentric orbit ($P = 9.6$ d, $e = 0.43$; Fig. 9; Table 7). The circularisation time-scale for such a planet (e.g. eq. 3 of Adams & Laughlin 2006, and assuming $Q_P \sim 10^5$) would be of order 30 Gyr, and so the eccentricity is compatible with the old age of the star. Given the transit, the probability that there is also an occultation of the planet (using eq. 2 of Kane & von Braun 2009) is greater than 0.46.

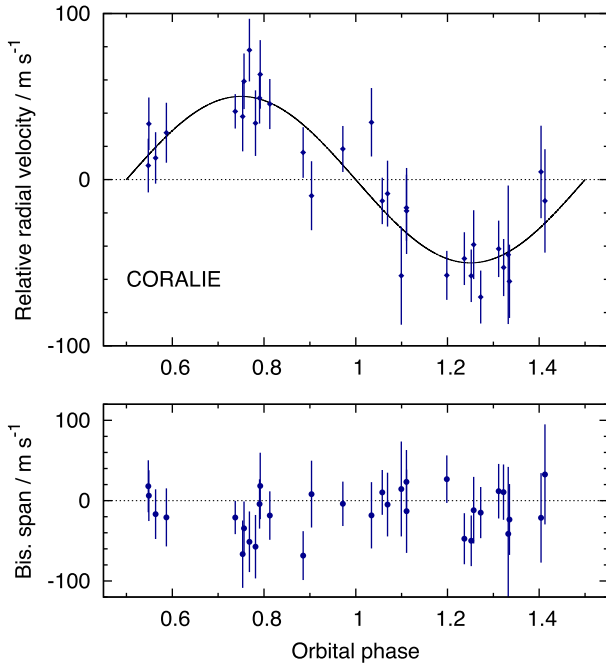**Figure 10.** WASP-168b discovery photometry, as for Fig. 2.

Figure 11. WASP-168b radial velocities and bisector spans, as for Fig. 3.

planetary radius is not well constrained. Nevertheless, the estimates give a bloated planet with a mass of $0.42 \pm 0.04\,M_{\rm Jup}$ and a radius of $1.5\,^{+0.5}_{-0.3}\,R_{\rm Jup}$. As noted for WASP-159b, bloated hot Jupiters with similar parameters are commonly found.

Table 8. System parameters for WASP-168.

1SWASP 062658.70–464917.1	
2MASS 06265871-4649171	
GAIA RA $= 06^{\rm h}26^{\rm m}58.71^{\rm s}$, Dec $= -46°49'17.2''$ (J2000)	
V mag $= 12.1$	
Rotational modulation <3 mmag (95%)	
UCAC5 pm (RA) 0.0 ± 1.1 (Dec) 20.1 ± 1.1 mas yr^{-1}	
GAIA parallax: 3.13 ± 0.25 mas	
Stellar parameters from spectroscopic analysis.	
Spectral type	F9V
$T_{\rm eff}$ (K)	$6\,000 \pm 100$
Log g	4.0 ± 0.1
$v \sin i$ (km s^{-1})	0.3 ± 0.1
[Fe/H]	-0.01 ± 0.09
Log A(Li)	2.93 ± 0.12
Age (Lithium) (Gyr)	<1
Parameters from MCMC analysis.	
P (d)	$4.153\,658 \pm 0.000\,003$
$T_{\rm c}$ (HJD) (UTC)	$2\,45\,7\,424.527\,8 \pm 0.000\,4$
T_{14} (d)	$0.079\,7 \pm 0.001\,7$
$T_{12} = T_{34}$ (d)	Undefined
$\Delta F = R_{\rm P}^2/R_*^2$	$0.011\,9\,^{+0.0015}_{-0.0007}$
b	$0.97\,^{+0.06}_{-0.04}$
i (°)	84.4 ± 0.6
K_1 (km s^{-1})	0.050 ± 0.004
γ (km s^{-1})	50.460 ± 0.003
e	0 (adopted) (< 0.09 at 2σ)
a/R_*	$9.59\,^{+0.65}_{-0.39}$
M_* (M$_\odot$)	1.08 ± 0.05
R_* (R$_\odot$)	1.12 ± 0.06
Log g_* (cgs)	4.37 ± 0.05
ρ_* ($\rho_\odot$)	0.77 ± 0.14
$T_{\rm eff}$ (K)	6000 ± 100
$M_{\rm P}$ ($M_{\rm Jup}$)	0.42 ± 0.04
$R_{\rm P}$ ($R_{\rm Jup}$)	$1.5\,^{+0.5}_{-0.3}$
log $g_{\rm P}$ (cgs)	2.6 ± 0.3
$\rho_{\rm P}$ ($\rho_{\rm J}$)	$0.12\,^{+0.10}_{-0.07}$
a (AU)	$0.051\,9 \pm 0.000\,8$
$T_{\rm P,A = 0}$ (K)	1340 ± 40

Note. Errors are 1σ; limb-darkening coefficients were:
r band: a1 $= 0.547$, a2 $= 0.084$, a3 $= 0.308$, a4 $= -0.215$.
z band: a1 $= 0.633$, a2 $= -0.263$, a3 $= 0.523$, a4 $= -0.280$.
V band: a1 $= 0.462$, a2 $= 0.310$, a3 $= 0.181$, a4 $= -0.170$.
I band: a1 $= 0.627$, a2 $= -0.208$, a3 $= 0.518$, a4 $= -0.286$.

12 WASP-172

WASP-172 is a fairly hot, F1 star with $V = 11.0$ and a metallicity of [Fe/H] $= -0.10 \pm 0.08$. The age estimate is 1.8 ± 0.3 Gyr. WASP-172b is a moderately bloated planet ($0.5\,M_{\rm Jup}$; $1.6\,R_{\rm Jup}$) in a 5.48-d orbit (Figs 12 and 13; Table 9).

The large stellar radius (1.9 R$_\odot$) leads to a small transit depth of 0.7 per cent and thus a ground-based survey would struggle to have detected the planet if it were not bloated. Thus, while highly irradiated hot Jupiters around hot stars are often found to be bloated, one has to be careful with observational biases in constructing such samples.

13 WASP-173

WASP-173A (Figs 14 and 15; Table 10) is the brighter component of a known double-star system catalogued as WDS23366 − 3437 (Mason et al. 2001). The two components have $V = 11.3$ and
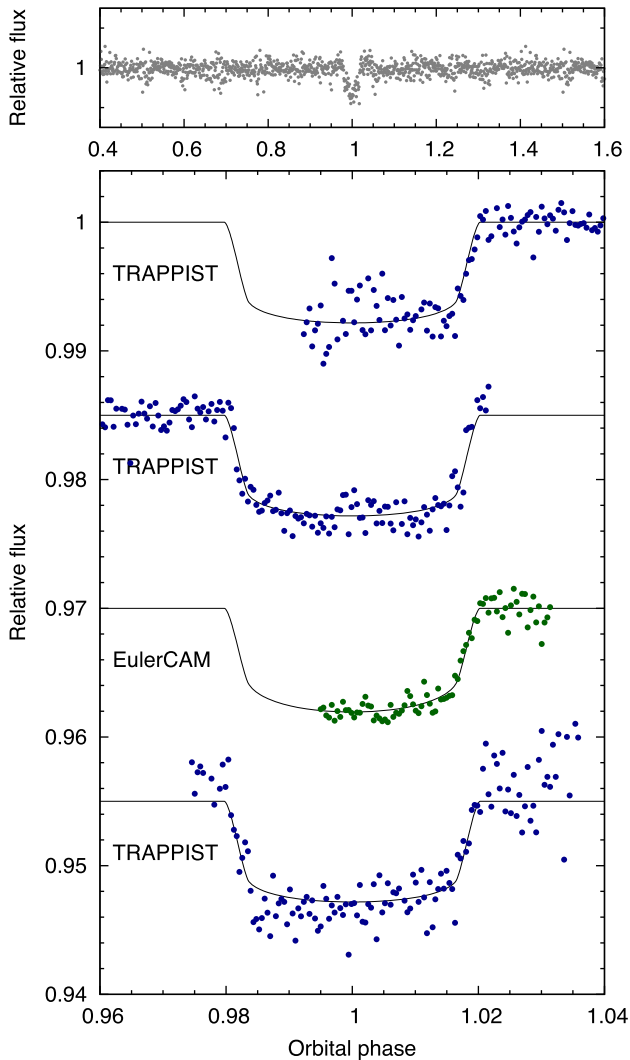
Figure 12. WASP-172b discovery photometry, as for Fig. 2.

Figure 13. WASP-172b radial velocities and bisector spans, as for Fig. 3.

12.1 and are separated by 6 arcsec. Given the GAIA parallax of 4.34 ± 0.61 mas, this amounts to a separation 1400 ± 200 AU. Our spectral analysis suggests a type of G3 and a metallicity of $+0.16 \pm 0.14$ for WASP-173A (we do not have spectra of the companion). The age estimate is 7 ± 3 Gyr.

The WASP data show a rotational modulation at a period of 7.9 ± 0.1 d (Fig. 16). It is seen independently in three seasons (2006, 2007, 2011), with false-alarm probabilities of <0.1 per cent in two of them. The amplitude ranges from 6 to 15 mmag. Given the 14-arcsec pixels of WASP data, we cannot tell which of the two stars is producing the modulation, but the amplitude suggests that it is more likely to be the brighter component, WASP-173A (note that the quoted amplitude has not been corrected for dilution). The follow-up transit light curves with EulerCAM and TRAPPIST-South used a smaller aperture containing only WASP-173A.

WASP-173Ab is a massive planet ($3.7\,M_{\rm Jup}$) in a close-in, circular orbit with a period of 1.39 d. The radius is $1.2\,R_{\rm Jup}$.

Given the stellar radius of 1.11 ± 0.05 $R_\odot$ the rotation period implies a surface velocity of 7.15 ± 0.35 km s^{-1}. This compares with the measured $v\sin i$ of 6.1 ± 0.3 km s^{-1}. This suggests that the spin axis might not be fully perpendicular to us, and thus that the planet might be in a m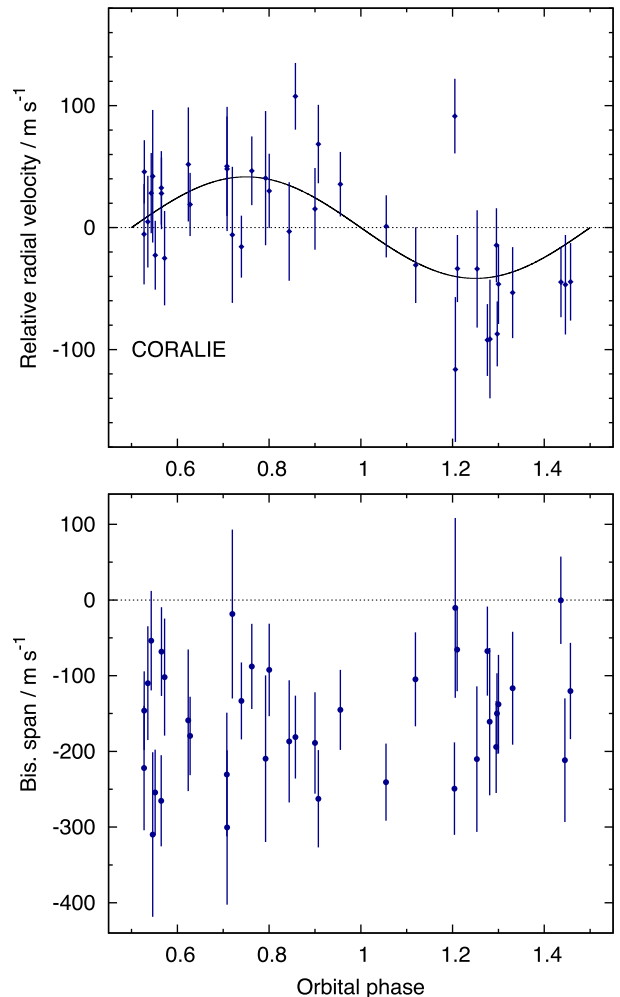oderately misaligned orbit. This system may be a worthwhile target for an observation of the Rossiter–McLaughlin effect.

14 DISCUSSION

To illustrate the newly discovered hot-Jupiter systems, we plot some of their properties in Fig. 17. Blue symbols indicate the objects reported here; red symbols are from other recent WASP discovery papers (Anderson et al. 2018a; Barkaoui et al. 2018; Demangeon et al. 2018; Lendl et al. 2018; Temple et al. 2018), while grey symbols are objects from the literature, including the recent HATSouth paper, Hartman et al. (2018).

The figure illustrates that the new systems lie within known parameter space, while being well distributed within the space. As is well established, the more massive planets are less likely to be highly bloated (top panel). The upper bound of planet radius in this plot is likely real while the lower bound could well involve selection effects, since smaller planets are harder to find in ground-based transit surveys, though whether this is the case will be established by the *TESS* survey. In common with past findings (e.g. Petigura et al. 2018), hot Jupiters are preferentially found around metal-rich stars (middle panel). The lower panel shows the marked decline in the hot Jupiter population at periods above 5–6 d (e.g. Hellier et al. 2017) which is too marked to be purely a selection effect

Table 9. System parameters for WASP-172.

1SWASP 131744.13–471415.3	
2MASS 13174412–4714152	
GAIA RA = $13^h17^m44.12^s$, Dec = $-47°14'15.3''$ (J2000)	
V mag = 11.0	
Rotational modulation: <1 mmag (95%)	
UCAC5 pm (RA) -16.2 ± 0.8 (Dec) 0.7 ± 0.8 mas yr^{-1}	
GAIA parallax: 1.78 ± 0.26 mas	

Stellar parameters from spectroscopic analysis.

Spectral type	F1V
T_{eff} (K)	$6\,900 \pm 150$
Log g	4.1 ± 0.2
$v \sin i$ (km s^{-1})	13.7 ± 1.0
[Fe/H]	-0.10 ± 0.08
log A(Li)	<1.2
Age (Lithium) (Gyr)	(Too hot for estimate)

Parameters from MCMC analysis.

P (d)	$5.477\,433 \pm 0.000\,007$
T_c (HJD) (UTC)	$2\,45\,7\,032.261\,7 \pm 0.000\,5$
T_{14} (d)	$0.220\,6 \pm 0.002\,0$
$T_{12} = T_{34}$ (d)	0.021 ± 0.002
$\Delta F = R_P^2/R_*^2$	$0.007\,2 \pm 0.000\,2$
b	0.45 ± 0.12
i (°)	86.7 ± 1.1
K_1 (km s^{-1})	0.042 ± 0.009
γ (km s^{-1})	-20.283 ± 0.006
e	0 (adopted) (<0.28 at 2σ)
a/R_*	8.0 ± 0.5
M_* (M$_\odot$)	1.49 ± 0.07
R_* (R$_\odot$)	1.91 ± 0.10
Log g_* (cgs)	4.05 ± 0.05
ρ_* ($\rho_\odot$)	0.21 ± 0.04
T_{eff} (K)	$6\,900 \pm 140$
M_P (M_{Jup})	0.47 ± 0.10
R_P (R_{Jup})	1.57 ± 0.10
Log g_P (cgs)	2.64 ± 0.11
ρ_P (ρ_J)	0.12 ± 0.04
a (AU)	$0.069\,4 \pm 0.001\,1$
$T_{P, A=0}$ (K)	1740 ± 60

Note. Errors are 1σ; limb-darkening coefficients were:
r band: a1 = 0.422, a2 = 0.603, a3 = -0.477, a4 = 0.129.
z band: a1 = 0.513, a2 = 0.159, a3 = -0.089, a4 = -0.018.

caused by longer-period systems producing fewer transits and so being harder to find. The ongoing WASP survey is thus continuing to add to the statistics of the population, while finding some systems with exceptional properties (e.g. WASP-128b, Hodžić et al. 2018; WASP-189b, Anderson et al. 2018b), and adding to the number of hot Jupiters transiting stars bright enough to allow atmospheric characterisation (e.g. Nikolov et al. 2018; Spake et al. 2018).

With regards to atmospheric characterization, the most promising of the new targets presented here is WASP-172b. This is a bloated, low-mass hot Jupiter (0.47 M_{Jup}; 1.57 R_{Jup}) transiting a relatively bright star at V = 11.0. The atmosphere is also predicted to be hot (1740 $\pm$ 60 K) owing to the hot, F1 host star. Other bloated planets in this batch are WASP-159b, with a fainter host of V = 12.9, and WASP-168b, which has both a fainter host with V = 12.1 and a grazing transit making it harder to parametrize.

WASP-144b is notable for being unbloated (R = 0.85 $\pm$ 0.05 R_{Jup}). WASP-145b may also be unusually small for a hot Jupiter, but the radius has a large uncertainty owing to the transit being grazing.

Three of the planets reported here are relatively massive, WASP-158b at 2.8 M_{Jup}, WASP-173Ab at 3.7 M_{Jup}, and WASP-162b at 5.2
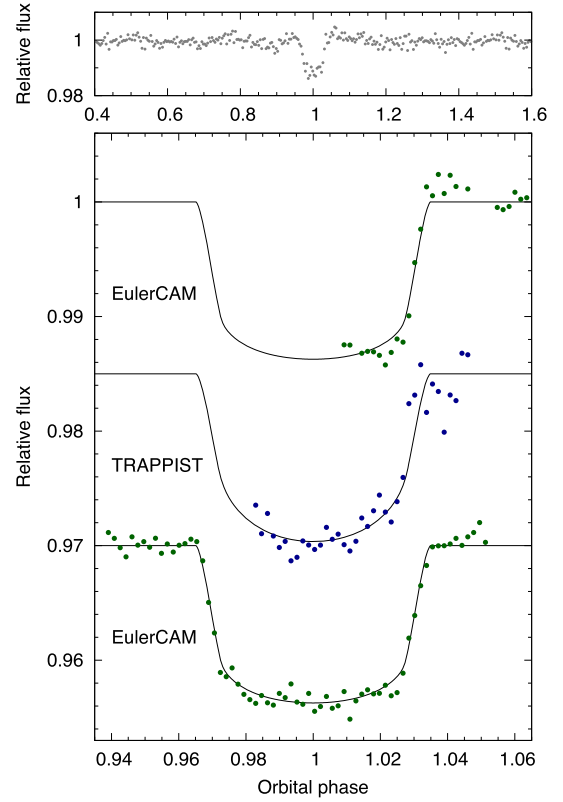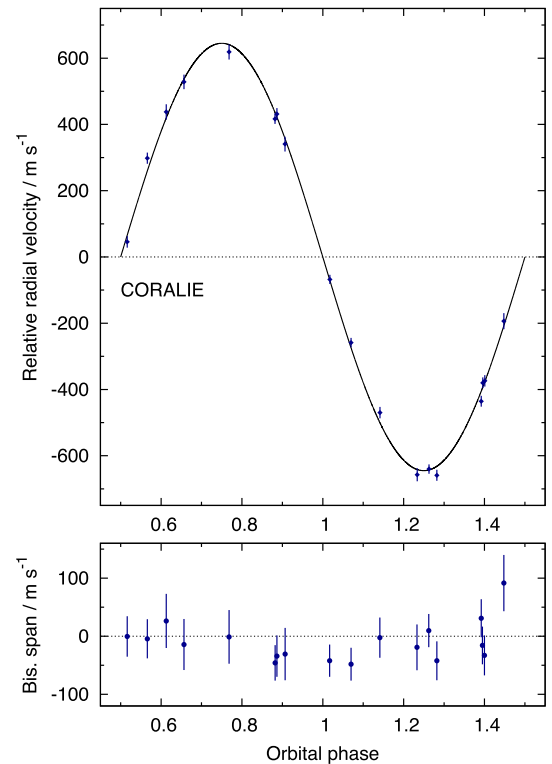

Figure 14. WASP-173b discovery photometry, as for Fig. 2.

Figure 15. WASP-173b radial velocities and bisector spans, as for Fig. 3.

Table 10. System parameters for WASP-173.

1SWASP 233640.32−343640.4	
2MASS 23364036−3436404	
WDS23366 − 3437	
GAIA RA = $23^h36^m40.38^s$, Dec = $−34°36'40.6''$ (J2000)	
V mag = 11.3	
Rotational modulation: $P = 7.9 \pm 0.1$; 6 − 15 mmag amplitude	
UCAC5 pm (RA) 88.1 ± 0.8 (Dec) $−8.3 \pm 0.8$ mas yr^{-1}	
GAIA parallax: 4.34 ± 0.61 mas	
Stellar parameters from spectroscopic analysis.	
Spectral type	G3
T_{eff} (K)	$5\,700 \pm 150$
Log g	4.5 ± 0.2
$v \sin i$ (km s^{-1})	6.1 ± 0.3
[Fe/H]	$+0.16 \pm 0.14$
Log A(Li)	<0.8
Age (Lithium) (Gyr)	>5
Parameters from MCMC analysis.	
P (d)	$1.386\,653\,18 \pm 0.000\,000\,27$
T_c (HJD) (UTC)	$2\,457\,288.858\,5 \pm 0.000\,2$
T_{14} (d)	$0.095\,7 \pm 0.000\,7$
$T_{12} = T_{34}$ (d)	$0.011\,7 \pm 0.000\,9$
$\Delta F = R_p^2/R_*^2$	$0.012\,3 \pm 0.000\,2$
b	0.40 ± 0.08
i (°)	85.2 ± 1.1
K_1 (km s^{-1})	0.645 ± 0.007
γ (km s^{-1})	$−7.858 \pm 0.004$
e	0 (adopted) (<0.032 at 2σ)
a/R_*	4.78 ± 0.17
M_* (M$_\odot$)	1.05 ± 0.08
R_* (R$_\odot$)	1.11 ± 0.05
Log g_* (cgs)	4.37 ± 0.03
ρ_* ($\rho_\odot$)	0.76 ± 0.08
T_{eff} (K)	$5\,800 \pm 140$
M_P (M_{Jup})	3.69 ± 0.18
R_P (R_{Jup})	1.20 ± 0.06
Log g_P (cgs)	3.77 ± 0.04
ρ_P (ρ_J)	2.14 ± 0.28
a (AU)	$0.024\,8 \pm 0.000\,6$
$T_{P, A = 0}$ (K)	$1\,880 \pm 55$

Note. Errors are 1σ; limb-darkening coefficients were:
r band: a1 = 0.673, a2 = −0.360, a3 = 0.893, a4 = −0.448.
z band: a1 = 0.754, a2 = −0.625, a3 = 0.957, a4 = −0.442.
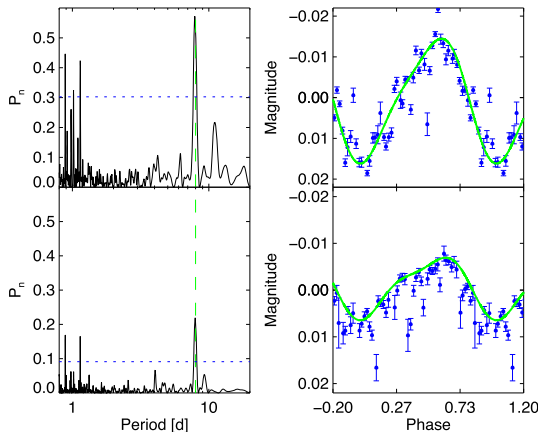V band: a1 = 0.602, a2 = −0.228, a3 = 0.902, a4 = −0.459.

Figure 16. WASP-173 rotational modulation. The left-hand panels show periodograms for independent WASP data sets from 2007 and 2011. The blue dotted line is a false-alarm probability of 0.001. The right-hand panels show the data for each season folded on the 7.9-d period; the green line is a harmonic-series fit to the data.
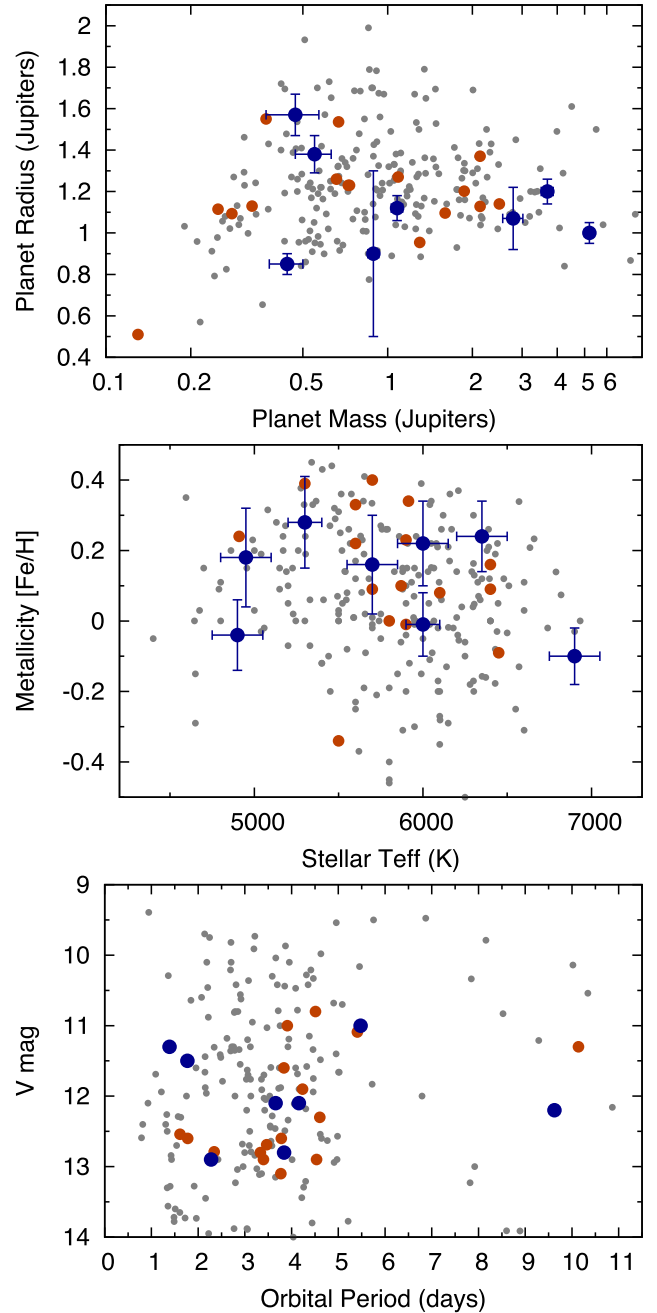
Figure 17. The new hot-Jupiter systems reported here (blue symbols) compared to recent WASP discoveries (red symbols) and previously known systems from the literature (grey). The figure shows planetary mass, radius, and orbital period along with host-star temperature, metallicity and V-band magnitude.

M_{Jup}. Such planets are relatively less common. Before this paper, only 21 transiting hot Jupiters were known with masses in the range 2.5–6 M_{Jup} compared to 205 in the range 0.5–2.5 M_{Jup}. Of the three new massive planets, only WASP-162b has a significant eccentricity ($e = 0.43$). Indeed WASP-173Ab is unusual in being a massive planet with no significant eccentricity (<0.032 at 2σ confidence), although this has likely explained its short orbital period (1.39 d) leading to enhanced circularisation torques (e.g. Adams & Laughlin 2006).

Two of the planets reported here (WASP-145Ab and WASP-173Ab) are in double-star systems, adding to other recent WASP discoveries in binary systems (e.g. WASP-160Bb; Lendl et al. 2018). This is partly a result of WASP paying closer attention to candidates in binaries that were ignored earlier in the project as being harder to observe. Overall, our results here show that the combination of WASP-South, CORALIE, and TRAPPIST-South continues to be a productive team for discovering hot Jupiters transiting stars of $V < 13$.

REFERENCES

Adams F. C., Laughlin G., 2006, ApJ, 649, 1004
Anderson D. R. et al., 2012, MNRAS, 422, 1988
Anderson D. R. et al., 2018a, preprint (arXiv:1809.07709)
Anderson D. R. et al., 2018b, preprint (arXiv:1809.04897)
Barkaoui K. et al., 2018, preprint (arXiv:1807.06548)
Barros S. C. C. et al., 2011, A&A, 525, A54
Bayliss D. et al., 2017, MNRAS, 475, 4467
Bean J. L. et al., 2018, PASP, 130, 114402
Claret A., 2000, A&A, 363, 1081
Collier Cameron A. et al., 2007a, MNRAS, 375, 951
Collier Cameron A. et al., 2007b, MNRAS, 380, 1230
Demangeon O. D. S. et al., 2018, A&A, 610, A63
Doyle A. P. et al., 2013, MNRAS, 428, 3164
Doyle A. P., Davies G. R., Smalley B., Chaplin W. J., Elsworth Y., 2014, MNRAS, 444, 3592
Gaia Collaboration et al., 2016, A&A, 595, A2
Gillon M. et al., 2013, A&A, 552, A82
Hartman J. D. et al., 2018, preprint (arXiv:1809.01048)
Hébrard G. et al., 2013a, A&A, 549, A134
Hébrard G. et al., 2013b, A&A, 554, A114
Hellier C. et al., 2014, MNRAS, 440, 1982
Hellier C. et al., 2017, MNRAS, 465, 3693
Henning T. et al., 2018, AJ, 155, 79
Hodžić V. et al., 2018, MNRAS, 481, 5091
Johnson M. C. et al., 2018, AJ, 155, 100
Kane S. R., von Braun K., 2009, PASP, 121, 1096
Lendl M. et al., 2012, A&A, 544, A72
Lendl M. et al., 2018, MNRAS, 482, 301
Mason B. D., Wycoff G. L., Hartkopf W. I., Douglass G. G., Worley C. E., 2001, AJ, 122, 3466
Maxted P. F. L. et al., 2011, PASP, 123, 547
Maxted P. F. L., Serenelli A. M., Southworth J., 2015, A&A, 575, A36
Maxted P. F. L. et al., 2016, A&A, 591, A55
Nikolov N. et al., 2018, Nature, 557, 526
Petigura E. A. et al., 2018, AJ, 155, 89
Pollacco D. L. et al., 2006, PASP, 118, 1407
Queloz D. et al., 2010, A&A, 517, L1
Ricker G. R. et al., 2016, in MacEwen H. A., Fazio G. G., Lystrup M., eds, Proc. SPIE Conf. Ser. Vol. 9904, Space Telescopes and Instrumentation 2016: Optical, Infrared, and Millimeter Wave. SPIE, Bellingham, p. 99042B
Santerne A., Bonomo A. S., Hébrard G., Deleuil M., Moutou C., Almenara J.-M., Bouchy F., Díaz R. F., 2011, A&A, 536, A70
Sestito P., Randich S., 2005, A&A, 442, 615
Smith A. M. S. et al., 2012, AJ, 143, 81
Spake J. J. et al., 2018, Nature, 557, 68
Talens G. J. J. et al., 2017, A&A, 606, A73
Temple L. Y. et al., 2018, MNRAS, 480, 5307
Triaud A. H. M. J. et al., 2013, A&A, 551, A80
Weiss A., Schlattl H., 2008, Ap&SS, 316, 99
Zacharias N., Finch C., Frouard J., 2017, AJ, 153, 166

SUPPORTING INFORMATION

Supplementary data are available at *MNRAS* online.

Table A1. Radial velocities.

Please note: Oxford University Press is not responsible for the content or functionality of any supporting materials supplied by the authors. Any queries (other than missing material) should be directed to the corresponding author for the article.

APPENDIX A

Table A1. Radial velocities. A full version of this table is available online.

BJD − 2400 000 (UTC)	RV (km s^{-1})	σ_{RV} (km s^{-1})	Bisector (km s^{-1})
WASP-144:			
56837.74442	16.1865	0.0468	− 0.0628
56845.73476	16.0438	0.0282	− 0.0215
56926.63966	16.1629	0.0189	0.0062
56927.64776	16.0215	0.0220	0.0326
56928.60109	16.1807	0.0241	0.1021
56930.71731	16.1352	0.0244	0.1589
56931.73201	16.0526	0.0324	0.0036
56942.60950	16.2039	0.0271	0.0623
56955.60807	16.1140	0.0251	− 0.0947
56958.62456	16.1967	0.0474	− 0.0913

This paper has been typeset from a TeX/LaTeX file prepared by the author.